


**COVER PAGE**

***Document downloaded by @DAEL***

***Fri Nov 27 04:12:32 2026***
***For personal use***

When automatic English translation is provided, only the original document is authentic.
The EAA cannot be held responsible of any translation error

Bibliographical reference

*Free Vibration Analysis of Single-Walled Carbon Nanotubes Based on the Nonlocal Higher-Order Cylindrical Beam Model*, Han Wen, Min-Fan He, Yong Huang and Jian Chen, Acta Acustica **vol. 104** (Number 2), 2018, pp. 284-294

DOI
https://doi.org/10.3813/AAA.919171

**Acta Acustica united with Acustica**
**Vol. 104 (2018) 284 – 294**

DOI 10.3813/AAA.919171

# Free Vibration Analysis of Single-Walled Carbon Nanotubes Based on the Nonlocal Higher-Order Cylindrical Beam Model

Han Wen, Min-Fan He, Yong Huang, Jian Chen
Department of Mathematics, Foshan University, Foshan, Guangdong 528000, China. hyhy1223@hotmail.com

**Summary**
In this paper, the free vibration behavior of single-walled carbon nanotubes (SWCNTs) is presented via a higher-order theory of nonlocal elastic cylindrical beams by taking the rotary inertia, shear deformation and small scale effect into account simultaneously. In our model, the shear-free surface condition is identically satisfied and does not need to introduce the shear correction factor. The characteristic equations of natural frequencies and the expressions of vibration mode shapes are derived in closed form for different boundary conditions. Compared our numerical results with those obtained by the molecular dynamics simulation, the effectiveness and validity of the present model are examined. The effects of the length-to-diameter ratio, the scale coefficient, the Poisson's ratio, chirality and boundary conditions on the free vibration of SWCNTs are investigated.

**PACS no. 43.40.Cw**

## 1. Introduction

Since the discovery of carbon nanotubes by Iijima in 1991 [1], nanostructures have attracted increasing attention of researchers in recent years due to their many unique properties [2], such as low weight, the superhigh-tensile stiffness, failure strength, and thermal and electrical conductivities, and so on. Generally speaking, the theoretical approaches in studying the mechanical properties of carbon nanotubes may be classified in two categories. One is based on the atomistic modelling or molecular dynamics simulation [3]–[5]. The second approach is to model nanostructures by using continuum mechanics that assume carbon nanotubes be a continuum or composed of continuum structures [6]–[8], which can be classified into classical continuum mechanics and nonclassical continuum mechanics. Because of the computational efficiency and simplicity, the continuum mechanics approach is widely used in simulating the mechanical behaviors of carbon nanotubes compared with the atomistic approach. However, the classical continuum theories don't incorporate the small scale effect into the model so that they can not describe the size effect in the analysis. Based on the nonlocal continuum theory introduced by Eringen [9]–[10], Peddieson *et al.* first suggested using this theory to characterize carbon nanotubes with the size effect considered [11]. Since then, there are many studies related to the static, wave propagation, vibration and buckling analysis of carbon nanotubes by using the nonlocal elasticity concept [12]–[16].

It is well-known that the the nonlocal continuum theory models relative to nano-tube may be classified to two categories. One is based on three dimensional elasticity theory or shell model, which and the final governing equation involve three or two at least spatial coordinates. Although this approach provides a quite adequate description of the problem, it needs a complex manipulation. The second approach is to transform a three-dimensional elastic problem to a one-dimensional elastic problem based on the beam theory. As compared to the preceding method, the second approach is simpler and more feasible in engineering practice since only one spatial coordinate is involved. Till to now, there have been a large number of literatures devoted to free vibration of carbon nanotubes by using the latter approach. Based on theory of nonlocal elasticity and Euler-Bernoulli beam, a nonlocal double-elastic beam model has been used to analyze the free transverse vibrations of double-walled carbon nanotubes [17]. In [18], Lu *et al.* have discussed the dynamic properties of flexural nanobeam structures and derived the frequency equations and modal shape functions for simply supported, clamped, and cantilevered beam by using the nonlocal Euler-Bernoulli beam model. Eltaher *et al.* used the variational statement to derive the equations of motion for a nonlocal Euler–Bernoulli nanobeam, and then employed the finite element method to discretize the model and obtained a numerical approximation [19]. A nonlocal Rayleigh beam theory has been developed to investigate the vibration behavior of simply supported inclined single-walled carbon nanotubes conveying viscous fluids

Received 12 May 2017,
accepted 15 January 2018.


© S. Hirzel Verlag · EAA

flow [20]. Based on Eringen's nonlocal elasticity theory and the Timoshenko beam theory, Wang *et al.* derived the governing equations and the boundary conditions by using the Hamilton's principle, and then presented the expressions for natural frequencies and the modal shapes in closed form [21]. Making using of nonlocal Timoshenko beam theory, Li and Wang studied the effects of the nonlocal parameter on natural frequencies and modal shapes in detail [22]. Reddy [23] employed nonlocal elasticity theory and the various available beam theories, including the Euler–Bernoulli, Timoshenko, Reddy, and Levinson beam theories, to investigate the effect of the nonlocal behavior on deflections, buckling loads, and natural frequencies.

It is well known that the natural frequencies of free vibration of beams are always overestimated by the Euler–Bernoulli beam theory duo to the fact that it does't consider the effects of rotary inertia and shear deformation of cross sections. Although Rayleigh beam theory take into account the effect of the rotary inertia of cross sections, still neglects the shear deformation of cross sections. Timoshenko beam theory is a more accurate beam, model, where considers the effects of both the rotary inertia and shear deformation of cross sections. It should be noted that the Timoshenko beam theory must bring a new physical quantity in its model, named shear correction coefficient, to relax the traction-free condition on the surface. However, the shear correction coefficient can only determined by other theories or experimental approaches. Huang *et al.* [24] have built a high-order beam model for bending and free vibration of cylindrical beams with circular cross-section, where the rotary inertia and shear deformation are taken into account simultaneously. Moreover, this model does not require a shear correction factor. In [25], we have used this model and nonlocal elasticity theory to study the behavior of flexural waves traveling in carbon nanotubes in a free space and embedded in an elastic matrix, where the obtained numerical results are in very good agreement with those based on molecular dynamics simulation.

This paper is to propose a nonlocal higher-order cylindrical beam model for discussing the flexural vibration behavior of SWCNTs. In this model, the traction-free condition is satisfied at the circumferential surface of the beam. The governing equations are presented, and the exact analytical solutions of natural frequencies and mode shapes are derived with various end conditions. Our numerical results are compared with other results based on molecular dynamics simulation. The effects of some physical quantities on the free vibration of SWCNTs are studied.

## 2. Theoretical formulation

In this section, we will apply the high-order cylindrical beam model to derive the governing equations and relevant boundary conditions for free vibration of the SWCNTs. It should be noted that the transverse vibration is only concerned in this paper, and the circumferential vibration of the carbon nanotubes is neglected.

### 2.1. Governing equation

Based on the higher-order model for cylindrical beams with circular cross-section [24], the displacement fields can be expressed as

$$u = z\psi(x,t) - \frac{z^3 + zy^2}{3R^2}\left[\frac{\partial w(x,t)}{\partial x} + \psi(x,t)\right], \quad (1)$$

$$v = v(y,z,t), \quad (2)$$

$$w = w(x,t), \quad (3)$$

where $u$ and $v$ are the two displacement components in the $x$- and $y$-directions, respectively; $w$ and $\psi$ are the lateral deflection and the rotation angle, respectively; $R$ is the radius of circular cross-section of the carbon nanotube. Because of the cylindrical beams with circular cross section, the present longitudinal displacement $u$ is an function that depends upon all three spatial coordinates $x$, $y$, and $z$, while the component $u$ in the Timoshenko and other beams only depends on two spatial coordinates $x$ and $z$.

By using the kinematic relations, we can obtain the normal strain $\varepsilon_{xx}$ and shear strains $\gamma_{xy}, \gamma_{xz}$ as

$$\varepsilon_{xx} = \frac{\partial u}{\partial x} = z\frac{\partial \psi}{\partial x} - \frac{z^3 + zy^2}{3R^2}\left(\frac{\partial^2 w}{\partial x^2} + \frac{\partial \psi}{\partial x}\right), \quad (4)$$

$$\gamma_{xy} = \frac{\partial u}{\partial y} + \frac{\partial v}{\partial x} = -\frac{2zy}{3R^2}\left(\frac{\partial w}{\partial x} + \psi\right), \quad (5)$$

$$\gamma_{xz} = \frac{\partial u}{\partial z} + \frac{\partial w}{\partial x} = \frac{3R^2 - 3z^2 - y^2}{3R^2}\left(\frac{\partial w}{\partial x} + \psi\right). \quad (6)$$

Furthermore, if employing the radial coordinate $r$ and above relations, we can easily get the shear strain $\gamma_{xr}$,

$$\gamma_{xr} = \frac{1}{r}\left(z\frac{\partial u}{\partial z} + z\frac{\partial w}{\partial x} + y\frac{\partial u}{\partial y} + y\frac{\partial v}{\partial x}\right) = \frac{z}{R^2\sqrt{z^2+y^2}}\left(R^2 - z^2 - y^2\right)\left(\psi + \frac{\partial w}{\partial x}\right), \quad (7)$$

which indicates that the shear stress $\tau_{xr}$ is vanishing at the surface $y^2 + z^2 = R^2$, because of the constitutive relations $\tau_{xr} = G\gamma_{xr}$. Therefore, the present model identically satisfies the shear-free condition at the circumferential surface.

For an elastic material in the one-dimensional case, the constitutive relations can be expressed according to the nonlocal theory,

$$\sigma_{xx} - l^2\frac{\partial^2 \sigma_{xx}}{\partial x^2} = E\varepsilon_{xx}, \quad (8)$$

$$\tau_{xy} - l^2\frac{\partial^2 \tau_{xy}}{\partial x^2} = G\gamma_{xy}, \quad (9)$$

$$\tau_{xz} - l^2\frac{\partial^2 \tau_{xz}}{\partial x^2} = G\gamma_{xz}, \quad (10)$$

where $\sigma_{xx}$ is the normal stress; $\tau_{xy}, \tau_{xz}$ are the shear stresses; $E$ and $G$ are Young's modulus and shear modulus of the carbon nanotube, respectively; and $l = e_0 a$ is a small scale coefficient that incorporates the small scale effect, $e_0$ being a non-dimensional material constant, and

$a$ being an internal characteristic length that is taken as the C–C bond length in this paper. The small scale coefficient can be estimated by numerical simulations or experiments.

By neglecting the equilibrium equation along the $y$-direction, we have the following equilibrium equations based on the three dimensional elasticity,

$$\frac{\partial \sigma_{xx}}{\partial x} + \frac{\partial \tau_{xy}}{\partial y} + \frac{\partial \tau_{xz}}{\partial z} = \rho \frac{\partial^2 u}{\partial t^2}, \tag{11}$$

$$\frac{\partial \tau_{xz}}{\partial x} + \frac{\partial \tau_{yz}}{\partial y} + \frac{\partial \sigma_{zz}}{\partial z} = \rho \frac{\partial^2 w}{\partial t^2}, \tag{12}$$

where $\rho$ is the mass density of the nanotube. Now we multiply both sides of Equation (11) by $z$ and $(1 - l^2\partial^2/\partial x^2)$, and insert Equations (8)–(10) into Equation (11), and then integrate both sides over the cross-sectional area $A$, resulting in

$$\frac{EI}{6}\left(7\frac{\partial^2 \psi}{\partial x^2} - 2\frac{\partial^3 w}{\partial x^3}\right) - GA\left(\frac{\partial w}{\partial x} + \psi\right) = \frac{\rho I}{6}\left(1 - l^2\frac{\partial^2}{\partial x^2}\right)\left(7\frac{\partial^2 \psi}{\partial t^2} - 2\frac{\partial^3 w}{\partial x \partial t^2}\right), \tag{13}$$

where $I = \pi R^4/4$ is the second moment of the cross-sectional area. One the other hand, if multiplying both sides of Equation (12) by $(1 - l^2\partial^2/\partial x^2)$ and integrating both sides over the cross-sectional area $A$, one gets

$$\frac{2}{3}GA\left(\frac{\partial^2 w}{\partial x^2} + \frac{\partial \psi}{\partial x}\right) = \left(1 - l^2\frac{\partial^2}{\partial x^2}\right)\left(\rho A\frac{\partial^2 w}{\partial t^2} - q\right), \tag{14}$$

where $q$ is a distributed force loading on a lateral surface of the beam in the $z$-direction. From Equations (13) and (14), we can find that two coupled governing equations for the free transverse vibration behavior of SWCNTs have been derive based on the higher-order beam theory.

If introducing a new auxiliary function $F$, we can convert the obtained coupled equations to the simple form of a single governing equation. For this purpose, the $w$ and $\psi$ can be expressed as

$$w = F - \frac{7EI}{6GA}\frac{\partial^2 F}{\partial x^2} + \frac{7\rho I}{6GA}\left(1 - l^2\frac{\partial^2}{\partial x^2}\right)\frac{\partial^2 F}{\partial t^2}, \tag{15}$$

$$\psi = -\frac{\partial F}{\partial x} - \frac{EI}{3GA}\frac{\partial^3 F}{\partial x^3} + \frac{\rho I}{3GA}\left(1 - l^2\frac{\partial^2}{\partial x^2}\right)\frac{\partial^3 F}{\partial x \partial t^2}. \tag{16}$$

We can find that Equation (13) automatically satisfies when substituting (15) and (16) into Equation (13). If inserting two above equations into Equation (14), we will get a single governing equation in $F$ as

$$\left[1 + l^2\left(\frac{\rho}{E} + \frac{7\rho}{6G}\right)\frac{\partial^2}{\partial t^2} + l^4\frac{7\rho^2}{6GE}\frac{\partial^4}{\partial t^4}\right]\frac{\partial^4 F}{\partial x^4} - \left(\frac{\rho}{E} + \frac{7\rho}{6G} + \frac{l^2\rho A}{EI}\right)\frac{\partial^4 F}{\partial t^2 \partial x^2} - \frac{l^2 7\rho^2}{6GE}\frac{\partial^6 F}{\partial t^4 \partial x^2} + \left(\frac{\rho A}{EI}\frac{\partial^2}{\partial t^2} + \frac{7\rho^2}{6GE}\frac{\partial^4}{\partial t^4}\right)F = \frac{1}{EI}\left(1 - l^2\frac{\partial^2}{\partial x^2}\right)q. \tag{17}$$

Let us discuss several special cases. Firstly, we present the corresponding coupled governing equations of the nonlocal Timoshenko beam theory for comparison [22],

$$EI\frac{\partial^2 \psi}{\partial x^2} - \kappa AG\left(\frac{\partial w}{\partial x} + \psi\right) = \rho I\left(1 - l^2\frac{\partial^2}{\partial x^2}\right)\frac{\partial^2 \psi}{\partial t^2}, \tag{18}$$

$$\kappa AG\left(\frac{\partial^2 w}{\partial x^2} + \frac{\partial \psi}{\partial x}\right) = \rho A\left(1 - l^2\frac{\partial^2}{\partial x^2}\right)\frac{\partial^2 w}{\partial t^2} - \left(1 - l^2\frac{\partial^2}{\partial x^2}\right)q, \tag{19}$$

where $\kappa$ is the shear correction coefficient. The Timoshenko beam theory must bring the new physical quantity in its model due to the fact, because that it makes an assumption of shear stress being uniformly distributed at any cross-section. But the Timoshenko beam theory cannot obtain this parameter directly, which can be only determined through other theories or experimental approaches. In the introduced model, we need not make the assumption of the shear stress uniformly distributed and bring in the shear correction factor. For the coupled governing equations of (18) and (19), if taking

$$w = F - \frac{EI}{\kappa GA}\frac{\partial^2 F}{\partial x^2} + \frac{\rho I}{\kappa GA}\left(1 - l^2\frac{\partial^2}{\partial x^2}\right)\frac{\partial^2 F}{\partial t^2}, \tag{20}$$

$$\psi = -\frac{\partial F}{\partial x}, \tag{21}$$

we immediately obtain a single governing equation as

$$\left[1 + l^2\left(\frac{\rho}{E} + \frac{\rho}{\kappa G}\right)\frac{\partial^2}{\partial t^2} + l^4\frac{\rho^2}{\kappa GE}\frac{\partial^4}{\partial t^4}\right]\frac{\partial^4 F}{\partial x^4} - \left(\frac{\rho}{E} + \frac{\rho}{\kappa G} + \frac{l^2\rho A}{EI}\right)\frac{\partial^4 F}{\partial t^2 \partial x^2} - \frac{l^2\rho^2}{\kappa GE}\frac{\partial^6 F}{\partial t^4 \partial x^2} + \left(\frac{\rho A}{EI}\frac{\partial^2}{\partial t^2} + \frac{\rho^2}{\kappa GE}\frac{\partial^4}{\partial t^4}\right)F = \frac{1}{EI}\left(1 - l^2\frac{\partial^2}{\partial x^2}\right)q. \tag{22}$$

Comparing Equations (15)–(17) with Equations (20)–(22), one can find that two governing equations and the expression for $w$ are identical if letting $\kappa = 6/7$. However, it can be also found that the expression for $\psi$ in the present model is different from that based on nonlocal Timoshenko beams.

Then, if we ignore the contribution of shear deformation by setting the shear rigidity to be sufficiently high $G \to \infty$, the governing equation (17) becomes to

$$\left(1 + l^2\frac{\rho}{E}\frac{\partial^2}{\partial t^2}\right)\frac{\partial^4 F}{\partial x^4} - \left(\frac{\rho}{E} + \frac{l^2\rho A}{EI}\right)\frac{\partial^4 F}{\partial t^2 \partial x^2} + \frac{\rho A}{EI}\frac{\partial^2 F}{\partial t^2} = \frac{1}{EI}\left(1 - l^2\frac{\partial^2}{\partial x^2}\right)q, \tag{23}$$

which is identical to the governing equation based on the nonlocal Rayleigh beams [26]. Furthermore, if neglecting the rotary inertia and shear deformation, one get

$$\frac{\partial^4 F}{\partial x^4} - l^2\frac{\rho A}{EI}\frac{\partial^4 F}{\partial t^2 \partial x^2} + \frac{\rho A}{EI}\frac{\partial^2 F}{\partial t^2} = \frac{1}{EI}\left(1 - l^2\frac{\partial^2}{\partial x^2}\right)q, \tag{24}$$

which is identical to the governing equation by using the nonlocal Euler–Bernoulli theory. [17, 18].

### 2.2. Boundary conditions

In order to solve the governing equations (17) with the corresponding boundary conditions, we should give explicit expressions in terms of $F$ for bending moment $M$, shear force $Q$, rotation $\psi$ and the deflection $w$. First of all, we can find that $w$ and $\psi$ can be determined by Equations (15) and (16), respectively. One the other hand, the bending moment $M$ and shearing force $Q$ at any position $x$ of the beam can be evaluated through the following integrals

$$M = \int_A \sigma_{xx} z \, \mathrm{d}A, \tag{25}$$

$$Q = \int_A \tau_{xz} \, \mathrm{d}A. \tag{26}$$

With Equations (4)–(6) in mind, substitution of Equations (8)–(10) into Equations (25) and (26) results in

$$M - l^2 \frac{\partial^2 M}{\partial x^2} = \frac{EI}{9}\left(7\frac{\partial \psi}{\partial x} - 2\frac{\partial^2 w}{\partial x^2}\right), \tag{27}$$

$$Q - l^2 \frac{\partial^2 Q}{\partial x^2} = \frac{2GA}{3}\left(\frac{\partial w}{\partial x} + \psi\right). \tag{28}$$

Making use of the Equations (11)–(12) and (27)–(28), we can obtain

$$\frac{\partial M}{\partial x} - Q = \rho I\left(\frac{7}{9}\frac{\partial^2 \psi}{\partial t^2} - \frac{2}{9}\frac{\partial^3 w}{\partial x \partial t^2}\right), \tag{29}$$

$$\frac{\partial Q}{\partial x} + q = \rho A \frac{\partial^2 w}{\partial t^2}. \tag{30}$$

As a result, the expressions of the nonlocal bending moment $M$ and nonlocal shearing force $Q$ can be obtained by substituting Equations (29) and (30) into Equations (27) and (28) as

$$M = \frac{EI}{9}\left(7\frac{\partial \psi}{\partial x} - 2\frac{\partial^2 w}{\partial x^2}\right) + l^2\left[\rho I\left(\frac{7}{9}\frac{\partial^3 \psi}{\partial t^2 \partial x} - \frac{2}{9}\frac{\partial^4 w}{\partial t^2 \partial x^2}\right) + \rho A \frac{\partial^2 w}{\partial t^2} - q\right], \tag{31}$$

$$Q = \frac{2GA}{3}\left(\frac{\partial w}{\partial x} + \psi\right) \rho A \frac{\partial^2 w}{\partial t^2} + l^2\left(\rho A \frac{\partial^3 w}{\partial t^2 \partial x} - \frac{\partial q}{\partial x}\right). \tag{32}$$

Remembering (15) and (16) we can easily get the explicit expressions of bending moment $M$ and shear force $Q$ in terms of $F$. Therefore, all physical quantities corresponding to the boundary conditions can be expressed in terms of $F$ and its derivatives as

$$w = F - \frac{7EI}{6GA}\frac{\partial^2 F}{\partial x^2} + \frac{7\rho I}{6GA}\left(1 - l^2 \frac{\partial^2}{\partial x^2}\right)\frac{\partial^2 F}{\partial t^2}, \tag{33}$$

$$\psi = -\frac{\partial F}{\partial x} - \frac{EI}{3GA}\frac{\partial^3 F}{\partial x^3} + \frac{\rho I}{3GA}\left(1 - l^2 \frac{\partial^2}{\partial x^2}\right)\frac{\partial^3 F}{\partial x \partial t^2}, \tag{34}$$

$$M = l^2 \rho A\left[1 - \frac{7EI}{6GA}\frac{\partial^2}{\partial x^2} + \frac{7\rho I}{6GA}\left(1 - l^2 \frac{\partial^2}{\partial x^2}\right)\frac{\partial^2}{\partial t^2}\right]\frac{\partial^2 F}{\partial t^2} - EI\frac{\partial^2 F}{\partial x^2} - l^2\left(\rho c I \frac{\partial^4 F}{\partial x^2 \partial t^2} + q\right), \tag{35}$$

$$Q = l^2 \rho A\left[1 - \frac{7EI}{6GA}\frac{\partial^2}{\partial x^2} + \frac{7\rho I}{6GA}\left(1 - l^2 \frac{\partial^2}{\partial x^2}\right)\frac{\partial^2}{\partial t^2}\right]\frac{\partial^3 F}{\partial x \partial t^2} - EI\frac{\partial^3 F}{\partial x^3} + \rho I\left(1 - l^2 \frac{\partial^2}{\partial x^2}\right)\frac{\partial^3 F}{\partial x \partial t^2} - l^2 \frac{\partial q}{\partial x}. \tag{36}$$

Comparing Equations (33) to (36) with those based on the nonlocal Timoshenko(NT) beam[22], we can find that the expressions for $w$, $M$ and $Q$ in terms of $F$ are identical if $\kappa = 6/7$ for the two models. For this reason, there is no discrepancy between two solutions derived from the present theory and the Timoshenko beam theory with $\kappa = 6/7$ for some specific boundary conditions, such as a simply single-walled carbon nanotube.

## 3. Free vibration of the single-walled carbon nanotube

Now let us analyze the free vibration of the SWCNTs based on the higher-order cylindrical beam model. For this purpose, we can assume $q = 0$ and take the introduced auxiliary function $F$ as the form:

$$F(x) = f(x)\mathrm{e}^{\mathrm{i}\omega t}, \tag{37}$$

where $\omega$ is the circular frequency of free vibration. By putting the above into Equation (17), one can get,

$$B_1 \frac{\mathrm{d}^4 f(x)}{\mathrm{d}x^4} + B_2 \frac{\mathrm{d}^2 f(x)}{\mathrm{d}x^2} + B_3 f(x) = 0, \tag{38}$$

with

$$B_1 = 1 - \left(\frac{\rho}{E} + \frac{7\rho}{6G}\right) l^2\omega^2 + \frac{7\rho^2}{6GE} l^4 \omega^4,$$

$$B_2 = \frac{\rho A}{EI} l^2 \omega^2 - \frac{7\rho^2}{6GE} l^2 \omega^4 + \left(\frac{\rho}{E} + \frac{7\rho}{6G}\right)\omega^2,$$

$$B_3 = -\frac{\rho A}{EI}\omega^2 + \frac{7\rho^2}{6GE}\omega^4.$$

This is a forth-order ordinary differential equation with constant coefficients. By restricting to lower-order vibrational modes, a general solution to Equation (38) can be immediately obtained based on a standard approach for solving the above equation

$$f(x) = C_1 \cos(\lambda_1 x) + C_2 \sin(\lambda_1 x) + C_3 \cosh(\lambda_2 x) + C_4 \sinh(\lambda_2 x), \tag{39}$$

where $C_1, C_2, C_3$ and $C_4$ are unknown constants which can be determined from the boundary conditions, and

$$\lambda_{1,2} = \sqrt{\frac{\sqrt{B_2^2 - 4B_1B_3} \pm B_2}{2B_1}}. \tag{40}$$

Using the Equation (39), we can obtain the expressions of $M$, $Q$, $\varphi$ and $w$ as follows:

$$\begin{aligned} w &= C_1\alpha_1 \cos(\lambda_1 x) + C_2\alpha_1 \sin(\lambda_1 x) \\ &\quad + C_3\beta_1 \cosh(\lambda_2 x) + C_4\beta_1 \sinh(\lambda_2 x), \qquad (41) \\ \psi &= C_1\alpha_2 \sin(\lambda_1 x) - C_2\alpha_2 \cos(\lambda_1 x) \\ &\quad + C_3\beta_2 \sinh(\lambda_2 x) + C_4\beta_2 \cosh(\lambda_2 x), \qquad (42) \\ M &= C_1\alpha_3 \cos(\lambda_1 x) + C_2\alpha_3 \sin(\lambda_1 x) \\ &\quad + C_3\beta_3 \cosh(\lambda_2 x) + C_4\beta_3 \sinh(\lambda_2 x), \qquad (43) \\ Q &= C_1\alpha_4 \sin(\lambda_1 x) - C_2\alpha_4 \cos(\lambda_1 x) \\ &\quad + C_3\beta_4 \sinh(\lambda_2 x) + C_4\beta_4 \cosh(\lambda_2 x), \qquad (44) \end{aligned}$$

where

$$\begin{aligned} \alpha_1 &= 1 - \frac{7\rho I}{6GA}\omega^2 + \left(\frac{7EI}{6GA} - \frac{7\rho I}{6GA}\omega^2 l^2\right)\lambda_1^2, \\ \beta_1 &= 1 - \frac{7\rho I}{6GA}\omega^2 - \left(\frac{7EI}{6GA} - \frac{7\rho I}{6GA}\omega^2 l^2\right)\lambda_2^2, \qquad (45) \\ \alpha_2 &= \left(1 + \frac{1\rho I}{3GA}\omega^2\right)\lambda_1 \\ &\quad - \left(\frac{1EI}{3GA} - \frac{\rho I}{3GA}\omega^2 l^2\right)\lambda_1^3, \\ \beta_2 &= -\left(1 + \frac{1\rho I}{3GA}\omega^2\right)\lambda_2 \\ &\quad - \left(\frac{1EI}{3GA} - \frac{\rho I}{3GA}\omega^2 l^2\right)\lambda_2^3, \qquad (46) \\ \alpha_3 &= l^2\rho A\left(\frac{7\rho I}{6GA}\omega^4 - \omega^2\right) \\ &\quad - \left[l^2\rho A\left(\frac{7EI}{6GA}\omega^2 - \frac{7\rho I}{6GA}\omega^4 l^2\right)\right. \\ &\quad \left. - EI + l^2\rho I\omega^2\right]\lambda_1^2, \qquad (47) \\ \beta_3 &= l^2\rho A\left(\frac{7\rho I}{6GA}\omega^4 - \omega^2\right) \\ &\quad + \left[l^2\rho A\left(\frac{7EI}{6GA}\omega^2 - \frac{7\rho I}{6GA}\omega^4 l^2\right)\right. \\ &\quad \left. - EI + l^2\rho I\omega^2\right]\lambda_2^2, \qquad (48) \\ \alpha_4 &= \left[\rho I\omega^2 - l^2\rho A\left(\frac{7\rho I}{6GA}\omega^4 - \omega^2\right)\right]\lambda_1 \\ &\quad + \left[l^2\rho A\left(\frac{7EI}{6GA}\omega^2 - \frac{7\rho I}{6GA}\omega^4 l^2\right)\right. \\ &\quad \left. - EI + l^2\rho I\omega^2\right]\lambda_1^3, \qquad (49) \end{aligned}$$

$$\begin{aligned} \beta_4 &= -\left[\rho I\omega^2 - l^2\rho A\left(\frac{7\rho I}{6GA}\omega^4 - \omega^2\right)\right]\lambda_2 \\ &\quad + \left[l^2\rho A\left(\frac{7EI}{6GA}\omega^2 - \frac{7\rho I}{6GA}\omega^4 l^2\right)\right. \\ &\quad \left. - EI + l^2\rho I\omega^2\right]\lambda_2^3. \qquad (50) \end{aligned}$$

Combining the above formulas with the relevant boundary conditions, we can easily determine the natural frequencies and modal shapes of free vibration for the SWCNTs. Here we will present the explicit expressions of natural frequencies and modal shapes with different boundary conditions.

### 3.1. The simply-simply (SS) SWCNTs

First, let us consider a simply supported end at $x = 0$ and $x = L$, where the corresponding boundary conditions are

$$w(0) = M(0) = 0, \quad w(L) = M(L) = 0. \tag{51}$$

Substituting the expressions (41) and (43) for $w$ and $M$ into the above supported ends, we can get a system of linear equations for $C_j (j = 1, ..., 4)$ as

$$\mathbf{D}\left[C_1, C_2, C_3, C_4\right]^{\mathrm{T}} = 0, \tag{52}$$

where the superscript T denotes the transpose of a matrix, and

$$\mathbf{D} = \tag{53}$$
$$\begin{bmatrix} \alpha_1 & 0 & \beta_1 & 0 \\ \alpha_3 & 0 & \beta_3 & 0 \\ \alpha_1\cos(\lambda_1 L) & \alpha_1\sin(\lambda_1 L) & \beta_1\cosh(\lambda_2 L) & \beta_1\sinh(\lambda_2 L) \\ \alpha_3\cos(\lambda_1 L) & \alpha_3\sin(\lambda_1 L) & \beta_3\cosh(\lambda_2 L) & \beta_3\sinh(\lambda_2 L) \end{bmatrix}.$$

To obtain a nontrivial solution, the determinant of the coefficient matrix of the system has to vanish, i.e, $\det(\mathbf{D}) = 0$, which can be simplified as the following equation,

$$\sin(\lambda_1 L)\sinh(\lambda_2 L) = 0. \tag{54}$$

Solving Equation (54) results in $\lambda_n = n\pi/L (n = 1, 2, \ldots)$ and inserting it back into Equations (40), we can obtain the explicit expression for the natural frequencies of the simply single-walled carbon nanotubes,

$$\omega = \sqrt{\frac{\gamma_2 - \sqrt{\gamma_2^2 - 4\gamma_1}}{2\gamma_1}}, \tag{55}$$

with

$$\begin{aligned} \gamma_1 &= \frac{7\rho^2}{6GE}\left(l^4 + \frac{l^2}{\lambda_n^2} + \frac{1}{\lambda_n^4}\right), \\ \gamma_2 &= \left(\frac{\rho A}{EI}l^2 + \frac{\rho}{E} + \frac{7\rho}{6G}\right)\frac{1}{\lambda_n^2} + \left(\frac{\rho}{E} + \frac{7\rho}{6G}\right)l^2 + \frac{\rho A}{EI}\frac{1}{\lambda_n^4}. \end{aligned}$$

One the other hand, if substituting $\lambda_n = n\pi/L$ into the Equations (52) and (41), one immediately get the corresponding modal shapes for simply boundary condition as

$$w = \sin(\frac{n\pi}{L}x). \tag{56}$$

From the expressions for the natural frequencies (55) and the modal shapes (56), it can be easily found that the natural frequencies are affected by the scale effect parameter $l = e_0 a$. However, the modal shapes for simply ends are independent of the nonlocal parameter, which is indicated that the vibration mode shapes for nonlocal higher-order beam model are the same as the corresponding mode shapes for classic higher-order beams. This character has also been discovered based on the nonlocal Timoshenko beams [21] [22].

### 3.2. The clamped-simply (CS) SWCNTs

For the clamped-simply ends, the corresponding end conditions read:

$$w(0) = \psi(0) = 0, \quad w(L) = M(L) = 0. \tag{57}$$

Substituting (41)-(43) into (57), and using a procedure analogous to the above section, one can get the characteristic equation for natural frequency of clamped-simply SWCNTs as

$$\frac{\alpha_1\beta_2}{\alpha_2\beta_1}\tan(\lambda_1 L) + \tanh(\lambda_2 L) = 0. \tag{58}$$

Once the natural frequencies are solved by numerical approach, the modal shapes are be expressed as

$$\begin{aligned} w \;=\; & -\alpha_1\left[\cos(\lambda_1 x) - \cosh(\lambda_2 x)\right] \\ & + \alpha_1\left[\cos(\lambda_1 L) - \cosh(\lambda_2 L)\right] \\ & \cdot \frac{\frac{\alpha_1}{\alpha_2}\sin(\lambda_1 x) + \frac{\beta_1}{\beta_2}\sinh(\lambda_2 x)}{\frac{\alpha_1}{\alpha_2}\sin(\lambda_1 L) + \frac{\beta_1}{\beta_2}\sinh(\lambda_2 L)}. \end{aligned} \tag{59}$$

### 3.3. The clamped-clamped (CC) SWCNTs

The boundary conditions of clamped-clamped SWCNTs are specified by

$$w(0) = \psi(0) = 0, \quad w(L) = \psi(L) = 0. \tag{60}$$

By taking the general expressions (41) and 42 into the above boundary conditions, we can obtain the characteristic equation for natural frequency of clamped SWCNTs as

$$\begin{aligned} & 2\cos(\lambda_1 L)\cosh(\lambda_2 L) \\ & + \left(\frac{\alpha_1\beta_2}{\alpha_2\beta_1} - \frac{\alpha_2\beta_1}{\alpha_1\beta_2}\right)\sin(\lambda_1 L)\sinh(\lambda_2 L) \;=\; 2, \end{aligned} \tag{61}$$

and the vibration mode shapes as

$$\begin{aligned} w \;=\; & -\alpha_1\left[\cos(\lambda_1 x) - \cosh(\lambda_2 x)\right] \\ & + \alpha_1\left[\cos(\lambda_1 L) - \cosh(\lambda_2 L)\right] \\ & \cdot \frac{\frac{\alpha_1}{\alpha_2}\sin(\lambda_1 x) + \frac{\beta_1}{\beta_2}\sinh(\lambda_2 x)}{\frac{\alpha_1}{\alpha_2}\sin(\lambda_1 L) + \frac{\beta_1}{\beta_2}\sinh(\lambda_2 L)}. \end{aligned} \tag{62}$$

### 3.4. The clamped-free (CF) SWCNTs

For the case of clamped-free (cantilever) SWCNTs, the boundary conditions can be defined as

$$w(0) = \psi(0) = 0, \quad M(L) = Q(L) = 0. \tag{63}$$

Making use of Equations (41)–(44) as well as the above boundary conditions, after collection we can obtain the characteristic equation for natural frequency of cantilever SWCNTs as

$$\begin{aligned} & \left(\frac{\alpha_1\beta_3}{\alpha_2\beta_4} + \frac{\beta_1\alpha_3}{\beta_2\alpha_4}\right)\cos(\lambda_1 L)\cosh(\lambda_2 L) \\ & + \left(\frac{\alpha_1\alpha_3}{\alpha_2\alpha_4} - \frac{\beta_1\beta_3}{\beta_2\beta_4}\right)\sin(\lambda_1 L)\sinh(\lambda_2 L) \;=\; \frac{\alpha_1\beta_3}{\alpha_4\beta_2} + \frac{\beta_1\alpha_3}{\beta_4\alpha_2}, \end{aligned} \tag{64}$$

where the vibration mode shapes are defined as

$$\begin{aligned} w \;=\; & \alpha_1\left[\cos(\lambda_1 x) - \cosh(\lambda_2 x)\right] \\ & - \left[\alpha_3\cos(\lambda_1 L) - \alpha_1\frac{\beta_3}{\beta_1}\cosh(\lambda_2 L)\right] \\ & \cdot \frac{\frac{\alpha_1}{\alpha_2}\sin(\lambda_1 x) + \frac{\beta_1}{\beta_2}\sinh(\lambda_2 x)}{\frac{\alpha_3}{\alpha_2}\sin(\lambda_1 L) + \frac{\beta_3}{\beta_2}\sinh(\lambda_2 L)}. \end{aligned} \tag{65}$$

## 4. Numerical results and discussions

Based on the nonlocal higher-order cylindrical beam model, the lower natural frequencies and the corresponding vibration mode shapes can be easily obtained by solving the above characteristic equations with the aid of commercial software. In this section, we will employ the introduced method to analyze the free vibration behavior of the SWCNTs with different boundary conditions.

### 4.1. Model Validation

In order to examine the validity of the proposed model, let us first compare the present results of natural frequency $f_n = \omega_n/2\pi$ for SWCNTs with those available in literatures obtained by nonlocal Timoshenko (NT) beam model [27] and molecular dynamics (MD) simulation model [27] [28]. Based on second-generation reactive empirical bond-order potential, Zhang *et al.* [27] used the molecular dynamics simulation to investigate the vibration behavior of SWCNTS. The vibration characteristics of single- and double-walled carbon nanotubes have been researched in [28] by the use of molecular dynamics simulations based on the Tersoff-Brenner and Lennard-Jones potential energy functions. In this calculation, we consider a set of (5, 5) armchair SWCNTs of length-to-diameter ratios $L/d$ varying from 4.86 to 28.31, with the following mechanical parameters [27]: $E/\rho = 3.6481 \times 10^8 \mathrm{m}^2/\mathrm{s}^2$, Poisson's ratio $\nu = 0.19$, scale coefficient $e_0 = 1.25$, effective tube thickness $t = 0.066$nm. Evaluated results of first-order natural frequencies $f_1$ (THz) for free vibration of clamped-clamped SWCNTS and other exiting results are tabulated in Table I. Moreover, the relative errors between

Table I. First-order natural frequencies $f_1$ (THz) of CC (5, 5) armchair SWCNTS.

| $L/d$ | MD[28] | NT[27] | MD[27] | Present results | Relative errors |
|---|---|---|---|---|---|
| 4.86 | 1.1678 | 1.00309 | 1.06812 | 1.06474 | -0.32% |
| 6.67 | — | 0.61738 | 0.64697 | 0.64749 | 0.08% |
| 8.47 | 0.4924 | 0.41469 | 0.43335 | 0.43105 | -0.53% |
| 10.26 | — | 0.29634 | 0.30518 | 0.30607 | 0.29% |
| 13.89 | 0.1926 | 0.17012 | 0.18311 | 0.17439 | -4.76% |
| 17.49 | 0.1183 | 0.10993 | 0.11597 | 0.11226 | -3.20% |
| 21.06 | — | 0.07684 | 0.07629 | 0.07829 | 2.62% |
| 24.66 | — | 0.05649 | 0.05798 | 0.05750 | -0.83% |
| 28.31 | — | 0.04312 | 0.04578 | 0.04382 | -4.28% |

Table II. First three non-dimensional natural frequencies $\sqrt{\Omega_n}$ for SS and CS SWCNTS.

| | Simply-Simply support | | | | Clamped-Simply support | | | |
|---|---|---|---|---|---|---|---|---|
| $e_0a/L$ | $n=1$ | | $n=2$ | $n=3$ | $n=1$ | | $n=2$ | $n=3$ |
| 0 | 3.1060 | $3.0929^{NT}$ | 6.0256 | 8.6669 | 3.8127 | $3.7845^{NT}$ | 6.5901 | 9.0788 |
| 0.05 | 3.0871 | $3.0741^{NT}$ | 5.8848 | 8.2376 | 3.7863 | $3.7584^{NT}$ | 6.4297 | 8.6237 |
| 0.1 | 3.0337 | $3.0209^{NT}$ | 5.5432 | 7.3852 | 3.7124 | $3.6848^{NT}$ | 6.0431 | 7.7250 |
| 0.15 | 2.9541 | $2.9416^{NT}$ | 5.1386 | 6.5796 | 3.6032 | $2.5761^{NT}$ | 5.5903 | 6.8807 |
| 0.2 | 2.8580 | $2.8459^{NT}$ | 4.7534 | 5.9286 | 3.4733 | $2.4467^{NT}$ | 5.1636 | 6.2012 |
| 0.25 | 2.7544 | $2.7427^{NT}$ | 4.4145 | 5.4141 | 3.3350 | $3.3092^{NT}$ | 4.7916 | 5.6655 |
| 0.3 | 2.6496 | $2.6382^{NT}$ | 4.1241 | 5.0024 | 3.1971 | $3.1721^{NT}$ | 4.4746 | 5.2373 |
| 0.35 | 2.5477 | $2.5369^{NT}$ | 3.8761 | 4.6666 | 3.0648 | $3.0406^{NT}$ | 4.2050 | 4.8880 |
| 0.4 | 2.4509 | $2.4405^{NT}$ | 3.6632 | 4.3873 | 2.9408 | $2.9174^{NT}$ | 3.9741 | 4.5974 |
| 0.45 | 2.3603 | $2.3503^{NT}$ | 3.4790 | 4.1510 | 2.8258 | $2.8032^{NT}$ | 3.7747 | 4.3514 |
| 0.5 | 2.2761 | $2.2665^{NT}$ | 3.3182 | 3.9480 | 2.7199 | $2.6980^{NT}$ | 3.6006 | 4.1400 |

the present results and MD simulations [27] are also listed in Table I. Table I demonstrates that the present natural frequencies are in very good agreement with the above-mentioned results. The largest percentage of difference between the present results and MD simulations [27] is 4.76% for the ratio $L/d = 13.89$, which indicates that the nonlocal higher-order cylindrical beam model is very efficient in analyzing the free vibration of SWCNTS. The first three natural frequencies $f_n$ (THz) against length-to-diameter $L/d$ for cantilever SWCNTS are shown in Figure 1 based on the higher-order cylindrical beam model and MD simulations [27], respectively. From Figure 1 we can find that our results of first three natural frequencies for cantilever boundary condition are very close to those using molecular dynamics simulation [27]. It is also observed that the natural frequencies monotonically decrease with the increase in length-to-diameter ratios $L/d$, which indicates that the length-to-diameter ratios play an important role in determining the vibration behaviors of SWCNTs.

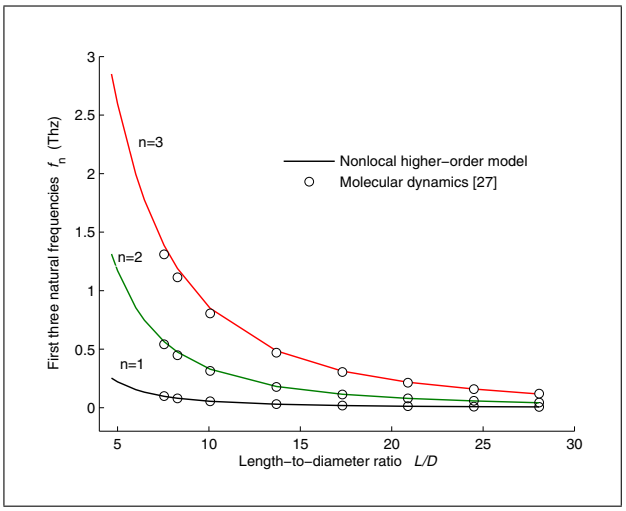


Figure 1. The first three natural frequencies $f_n$ (Thz) versus $L/d$ for a cantilever (5,5) armchair SWCNT based on the nonlocal higher-order beam theory and molecular dynamics simulation.

### 4.2. Effect of the scale parameter on the free vibration of SWCNTs

In this subsection, we will investigate the effect of the scale parameter on the natural frequencies and the vibration mode shapes. For this purpose, we consider (5, 5) armchair SWCNTs for SS and CS boundary conditions with lengths $L = 10d$ and the following mechanical properties: Poisson's ratio $\nu = 0.19$, effective tube thickness $t = 0.066$nm. Based on the characteristic Equations (55) and (57), we have calculated non-dimensional natural frequencies $\Omega_n = \omega L^2\sqrt{\rho A/EI}$ of SWCNTS for SS and CS boundary conditions. Evaluated results of first three non-dimensional frequency parameters $\sqrt{\Omega_n}$ are tabulated with different scale effect parameters in Table II. Based on

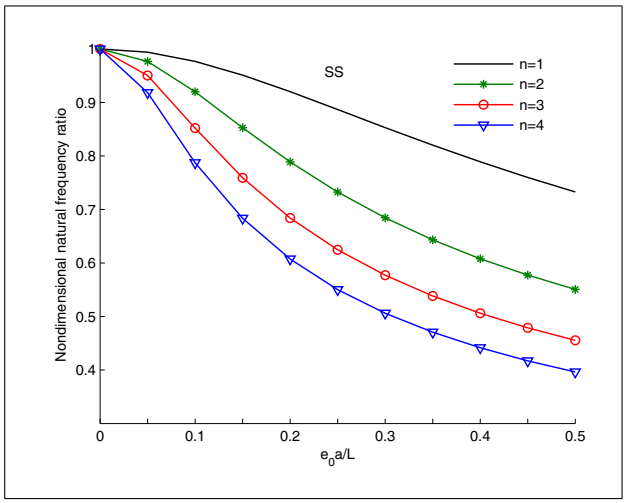


Figure 2. The non-dimensional natural frequencies ratio $\sqrt{\Omega_n}/\sqrt{\Omega_{n0}}$ versus the normalized scale effect parameter $e_0a/L$ for first four vibration modes with SS support.

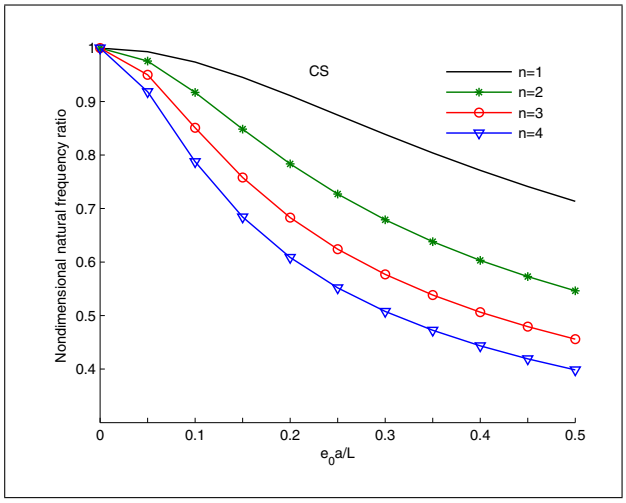


Figure 3. The non-dimensional natural frequencies ratio $\sqrt{\Omega_n}/\sqrt{\Omega_{n0}}$ versus the normalized scale effect parameter $e_0a/L$ for first four vibration modes with CS support.

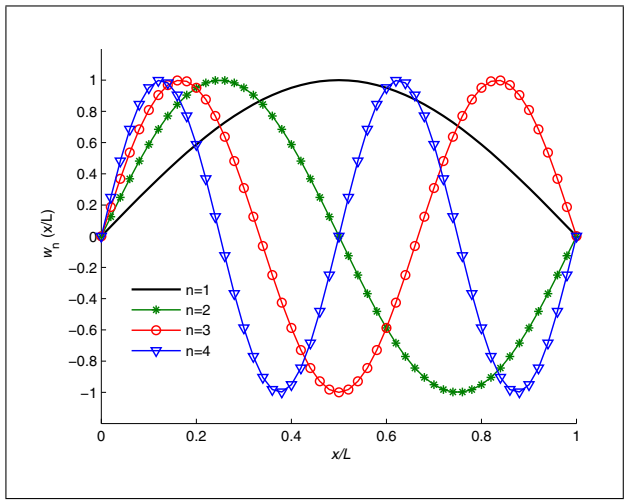


Figure 4. The first four vibration mode shapes of free vibration for simply boundary condition.

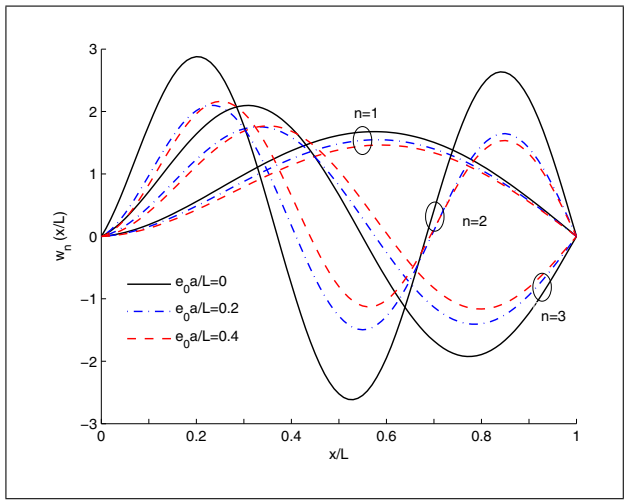


Figure 5. The first three vibration mode shapes of free vibration for clamped-simply boundary condition with different normalized scale effect parameters.

the nonlocal Timoshenko(NT) beam model[22], we have also calculated the first-order non-dimensional natural frequencies with $\kappa = 0.563$[21]. From Table II, it is seen that our numerical results are in agreement with those obtained by nonlocal Timoshenko beam model. Moreover, it can be observed that the natural frequencies decrease with the increase in normalized scale effect parameter $e_0a/L$ from Table II. The numerical results of $\sqrt{\Omega_n}$ for simply supports are less than that for CS supports, which has the same feature in the local beam theory. Therefore, scale effect parameters as well as end support conditions play a dominant role in determining natural frequencies. However, from Figures 2 and 3 we can find that the variation tendencies of the non-dimensional natural frequencies ratio $\sqrt{\Omega_n}/\sqrt{\Omega_{n0}}$ against the normalized scale effect parameter $e_0a/L$ are nearly identical for two boundary conditions. It should be noted that $\Omega_{n0}$ are the natural frequencies that calculated by letting $e_0a/L = 0$, which are corresponding to the results of local high-order beam theory. Furthermore, the effect of scale effect parameters on the vibration mode shapes for SS and CS boundary conditions is investigated and the results are plotted in Figures 4 and 5, respectively. Seen from Figure 4, the vibration mode shapes for simply boundary condition are independent of the scale effect parameters. Unlike the simply support, the shapes and amplitudes of vibrational modes for clamped-simply support are greatly influenced by the scale effect parameters, which can be found in Figure 5.

### 4.3. Effect of the Poisson's ratio on the free vibration of SWCNTs

In order to simulate the mechanical properties of SWCNTs, many different values of Poisson's ratio $\nu$ have been used in the published literatures, such as 0.19[21], 0.28[29], 0.3[30], and so on. On the basis of the obtained characteristic equations and the vibration mode shapes, we

Table III. First three non-dimensional natural frequencies $\sqrt{\Omega_n}$ for SWCNTS.

| | Clamped-Free support | | | Clamped-Clamped support | | |
|---|---|---|---|---|---|---|
| $\nu$ | $n=1$ | $n=2$ | $n=3$ | $n=1$ | $n=2$ | $n=3$ |
| 0.19 | 2.0887 | 4.4347 | 5.7556 | 4.0823 | 5.5202 | 6.4486 |
| 0.20 | 2.0886 | 4.4335 | 5.7529 | 4.0810 | 5.5173 | 6.4441 |
| 0.21 | 2.0884 | 4.4322 | 5.7501 | 4.0797 | 5.5145 | 6.4396 |
| 0.22 | 2.0883 | 4.4310 | 5.7474 | 4.0784 | 5.5116 | 6.4351 |
| 0.23 | 2.0881 | 4.4297 | 5.7447 | 4.0772 | 5.5088 | 6.4306 |
| 0.24 | 2.0879 | 4.4285 | 5.7420 | 4.0759 | 5.5059 | 6.4262 |
| 0.25 | 2.0878 | 4.4272 | 5.7393 | 4.0746 | 5.5031 | 6.4217 |
| 0.26 | 2.0876 | 4.4260 | 5.7366 | 4.0733 | 5.5003 | 6.4173 |
| 0.27 | 2.0874 | 4.4247 | 5.7339 | 4.0721 | 5.4975 | 6.4129 |
| 0.28 | 2.0873 | 4.4235 | 5.7312 | 4.0708 | 5.4947 | 6.4085 |
| 0.29 | 2.0871 | 4.4222 | 5.7285 | 4.0695 | 5.4919 | 6.4041 |
| 0.30 | 2.0869 | 4.4210 | 5.7258 | 4.0683 | 5.4891 | 6.3997 |

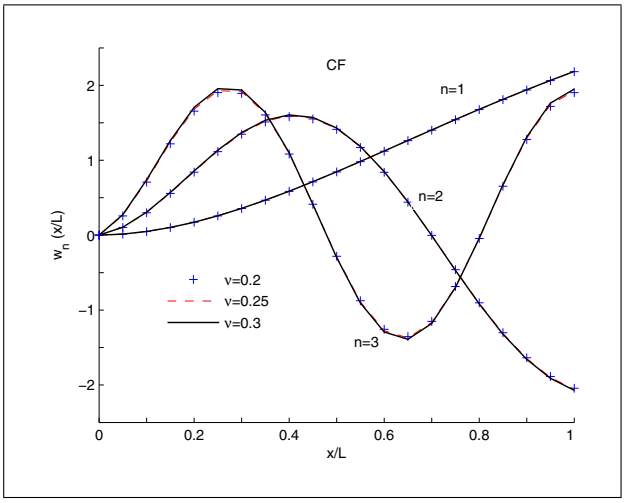


Figure 6. The variations of the vibration mode shapes $w_n$ with dimensionless coordinate $x/L$ for clamped-free boundary condition with different Poisson's ratios.

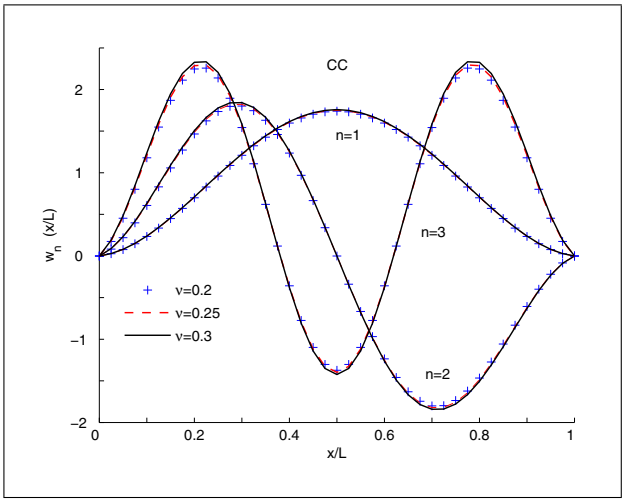


Figure 7. The variations of the vibration mode shapes $w_n$ with dimensionless coordinate $x/L$ for clamped-clamped boundary condition with different Poisson's ratios.

have investigated the effect of Poisson's ratio $\nu$ on the free vibration of (5, 5) armchair SWCNTs with the following mechanical properties: $L = 10d$, $t = 0.066$nm, $e_0a/L = 0.2$. The numerical results of first three non-dimensional natural frequencies $\sqrt{\Omega_n}$ are listed in Table III with clamped-clamped and clamped-free boundary conditions. From Table III, it is seen that the first three dimensionless natural frequencies decrease linearly with increasing Poisson's ratios $\nu$. Compared the results of $\nu = 0.19$ with $\nu = 0.3$, the largest percentage of differences between those are 0.52% and 0.76% for clamped-clamped and clamped-free supported ends, respectively. The variations of the vibration mode shapes $w_n$ with dimensionless coordinate $x/L$ are plotted in Figures 6 and 7 for two boundary conditions. It is observed that the vibration mode shapes are non-sensitive to the Poisson's ratio values. Therefore, it may be reasonable to conclude that the Poisson's ratio values have little influence on free vibration of SWCNTs.

### 4.4. Effect of chirality on the the free vibration of SWCNTs

In this subsection, we will study the possible role of chirality in the determining the natural frequencies and the vibration mode shapes of SWCNTs. For this purpose, we consider five chiral indices, namely, (5,5), (6,6), (7,7), (8,8), (9,9), (10,10), with the following mechanical properties: $L = 10d$, $\nu = 0.19$, $t = 0.066$nm, $e_0a/L = 0.2$. First three non-dimensional natural frequencies $\sqrt{\Omega_n}$ are calculated in Table IV based on the nonlocal higher-order beam model for CF, SS, CS and CC supported ends. In order to show the validity of our model, the results of first-order non-dimensional natural frequencies, which are calculated by nonlocal Timoshenko beam model with $\kappa = 0.563$[21], have also listed in Table IV. It is seen that the chirality has little influence on the first-order natural frequencies for CF and SS boundary conditions. However, this influence progressively becomes strong for higher-order vibration modes and other end supports. From Ta-

Table IV. First three non-dimensional natural frequencies $\sqrt{\Omega_n}$ for SWCNTS.

| End supports | $n$ | (5,5) | (6,6) | (7,7) | (8,8) | (9,9) | (10,10) |
|---|---|---|---|---|---|---|---|
| CF | 1 | 2.0887 | 2.0888 | 2.0888 | 2.0888 | 2.0889 | 2.0889 |
| | | $(2.0842)^{NT}$ | $(2.0843)^{NT}$ | $(2.0843)^{NT}$ | $(2.0844)^{NT}$ | $(2.0844)^{NT}$ | $(2.0844)^{NT}$ |
| | 2 | 4.4347 | 4.4352 | 4.4356 | 4.4358 | 4.4359 | 4.4360 |
| | 3 | 5.7556 | 5.7568 | 5.7575 | 5.7580 | 5.7583 | 5.7585 |
| SS | 1 | 2.8580 | 2.8581 | 2.8582 | 2.8582 | 2.8582 | 2.8583 |
| | | $(2.8459)^{NT}$ | $(2.8461)^{NT}$ | $(2.8462)^{NT}$ | $(2.8462)^{NT}$ | $(2.8462)^{NT}$ | $(2.8462)^{NT}$ |
| | 2 | 4.7534 | 4.7539 | 4.7542 | 4.7544 | 4.7545 | 4.7546 |
| | 3 | 5.9286 | 5.9298 | 5.9305 | 5.9310 | 5.9313 | 5.9315 |
| CS | 1 | 3.4733 | 3.4735 | 3.4737 | 3.4738 | 3.4738 | 3.4739 |
| | | $(3.4467)^{NT}$ | $(3.4471)^{NT}$ | $(3.4473)^{NT}$ | $(3.4474)^{NT}$ | $(3.4475)^{NT}$ | $(3.4475)^{NT}$ |
| | 2 | 5.1636 | 5.1645 | 5.1650 | 5.1653 | 5.1655 | 5.1657 |
| | 3 | 6.2012 | 6.2028 | 6.2037 | 6.2043 | 6.2047 | 6.2050 |
| CC | 1 | 4.0823 | 4.0828 | 4.0831 | 4.0832 | 4.0834 | 4.0835 |
| | | $(4.0357)^{NT}$ | $(4.0362)^{NT}$ | $(4.0366)^{NT}$ | $(4.0369)^{NT}$ | $(4.0370)^{NT}$ | $(4.0372)^{NT}$ |
| | 2 | 5.5202 | 5.5213 | 5.5220 | 5.5225 | 5.5228 | 5.5230 |
| | 3 | 6.4486 | 6.4504 | 6.4516 | 6.4524 | 6.4528 | 6.4532 |

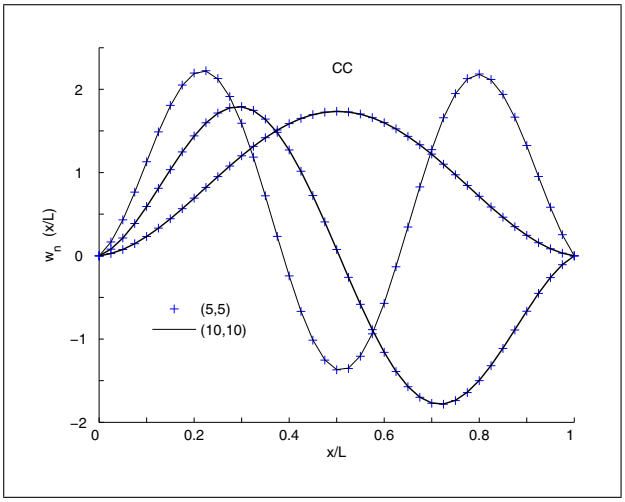


Figure 8. The variations of the vibration mode shapes $w_n$ with dimensionless coordinate $x/L$ for cantilever (5,5) and (10,10) SWCNTs.

ble IV it is clearly that the natural frequencies are sensitive to end support conditions. The first three vibration mode shapes for (5,5) and (10,10) SWCNTs with CC end support are plotted in Figure 8. Almost no difference in the vibration modes for both chiral indices can be observed from Figure 8.

## 5. Conclusions

By taking into account the effects of shear deformation, rotary inertia and size effect, a nonlocal higher-order cylindrical beam model has been applied to investigate the free vibration of SWCNTs. Based on this model, two coupled governing equations and the corresponding boundary conditions are derived. Then a single governing equation has been obtained by introducing an auxiliary function. Explicit expressions for natural frequencies and mode shapes of vibration have been presented with different boundary conditions. Our numerical results show excellent consistency with those of molecular dynamics simulation. The mode shapes for simply ends are independent of the nonlocal parameter. Through calculating the natural frequencies and modal shapes for each case, it is also found that the boundary conditions, the length-to-diameters and the scale parameter play an important role in determining the natural frequencies and mode shapes, while the Poisson's ratio values have little influence on free vibration of SWCNTs. The introduced model can be further extended to study other dynamic mechanical behaviors of SWCNTs.

### Acknowledgments

The authors would like to give their thanks to the financial support of the National Natural Science Foundation of China (Grant No. 11501106), Guangdong Provincial Natural Science Foundation of China (Grant No. 2016A030313835), Excellent Teacher Scheme in Guangdong Higher Education Institutions (No. Yq2014332, Yq2015164).

### References

[1] S. Iijima: Helical microtubules of graphitic carbon, Nature **354** (1991) 56–58.

[2] M. S. Dresselhaus, G. Dresselhaus, A. Jorio: Unusual properties and structure of carbon nanotubes, Annu. Rev. Mater. Res. **34** (2004) 247-278.

[3] A. Sears, R. C. Batra: Macroscopic properties of carbon nanotubes from molecular-mechanics simulations, Phys. Rev. B **69** (2004) 235406.

[4] A. Mashreghi, M. M. Moshksar: Investigating the effect of chirality on structural parameters of chiral single-walled carbon nanotubes by molecular dynamics simulation, Comput. Mater. Sci. **50** (2011) 934–938.

[5] C.L. Zhang, H. S. Shen: Buckling and postbuckling analysis of single-walled carbon nanotubes in thermal environments via molecular dynamics simulation, Carbon **44** (2006) 2608–2616.

[6] E. W. Wong, P. E. Sheehan, C. M. Lieber: Nanobeam mechanics: elasticity, strength, and toughness of nanorods and nanotubes, Science **277** (1997) 1971–1975.

[7] J. C. Hsu, R. P. Chang, W. J. Chang: Resonance frequency of chiral single-walled carbon nanotubes using Timoshenko beam theory, Phys. Lett. A **372** (2008) 2757–2759.

[8] M. M. Shokrieh, R. Rafiee: Prediction of Young's modulus of graphene sheets and carbon nanotubes using nanoscale continuum mechanics approach, Mater. Des. **31** (2010) 790–795.

[9] A. C. Eringen: On differential equations of nonlocal elasticity and solutions of screw dislocation and surface waves, J. Appl. Phys. **54** (1983) 4703.

[10] A. C. Eringen: Nonlocal Continuum Field Theories, Springer-Verlag, New York, 2002.

[11] J. Peddieson, G. R. Buchanan, R. P. McNitt: Application of nonlocal continuum models to nanotechnology, Int. J. Eng. Sci. **41** (2003) 305–312.

[12] Q. Wang: Wave propagation in carbon nanotubes via nonlocal continuum mechanics, J. Appl. Phys. **98** (2005) 124301.

[13] T. Murmu, S. C. Pradhan: Buckling analysis of a single-walled carbon nanotube embedded in an elastic medium based on nonlocal elasticity and Timoshenko beam theory and using DQM, Physica E **41** (2009) 1232–1239.

[14] J. N. Reddy, S. D. Pang: Nonlocal continuum theories of beams for the analysis of carbon nanotubes, J. Appl. Phys. **103** (2008) 023511.

[15] H. T. Thai, T. P. Vo: A nonlocal sinusoidal shear deformation beam theory with application to bending, buckling, and vibration of nanobeams, Int. J. Eng. Sci. **54** (2012) 58–66.

[16] S. L. Das, T. Mandal, S. S. Gupta: Inextensional vibration of zig-zag single-walled carbon nanotubes using nonlocal elasticity theories, Int. J. Solids Struct. **50** (2013) 2792–2797.

[17] Y. Q. Zhang, G. R. Liu, X. Y. Xie: Free transverse vibrations of double-walled carbon nanotubes using a theory of nonlocal elasticity, Phys. Rev. B **71** (2005) 195404.

[18] P. Lu, H. P. Lee, C. Lu, P. Q. Zhang: Dynamic properties of flxural beams using a nonlocal elasticity model, J. Appl. Phys. **99** (2006) 073510.

[19] M. A. Eltaher, A. E. Alshorbagy, F. F. Mahmoud: Vibration analysis of Euler-Bernoulli nanobeams by using finite element method, Appl. Math. Modell. **37** (2013) 4787–4797.

[20] K. Kiani: Vibration behavior of simply supported inclined single-walled carbon nanotubes conveying viscous fluids flow using nonlocal Rayleigh beam model, Appl. Math. Modell. **37** (2013) 1836–1850.

[21] C. M. Wang, Y. Y. Zhang, X. Q. He: Vibration of nonlocal Timoshenko beams, Nanotechnology **18** (2007) 105401.

[22] X. F. Li, B. L. Wang: Vibrational modes of Timoshenko beams at small scales, Appl. Phys. Lett. **94** (2009) 101903.

[23] J. N. Reddy: Nonlocal theories for bending, buckling and vibration of beams, Int. J. Eng. Sci. **45** (2007) 288–307.

[24] Y. Huang, J. X. Wu, X. F. Li, L. E. Yang: Higher-order theory for bending and vibration of beams with circular cross section, J. Eng. Math. **80** (2013) 91–104.

[25] Y. Huang, Q. Z. Luo, X. F. Li:, Transverse waves propagating in carbon nanotubes via a higher-order nonlocal beam model, Compos. Struct. **95** (2013) 328–336.

[26] J. X. Wu, X. F. Li, G. J. Tang: Bending wave propagation of carbon nanotubes in a bi-parameter elastic matrix, Phys. B. **407** (2012) 684–688.

[27] Y. Y. Zhang, C. M. Wang, V. B. C. Tan: Assessment of Timoshenko beam models for vibrational behavior of single-walled carbon nanotubes using molecular dynamics, Adv. Appl. Math. Mech. **1** (2009) 89-106.

[28] R. Ansari, S. Ajori, B. Arash: Vibrations of single- and double-walled carbon nanotubes with layer-wise boundary conditions: A molecular dynamics study, Current Appli. Phys. **12** (2012) 707-711.

[29] Z. B Shen, X. F. Li, L. P. Sheng, G. J. Tang: Transverse vibration of nanotube-based micro-mass sensor via nonlocal Timoshenko beam theory, Comput. Mater. Sci. **53** (2012) 340–346.

[30] L. Behera, S. Chakraverty: Application of differential quadrature method in free vibration analysis of nanobeams based on various nonlocal theories, Comput. Math. Appl. **69** (2015) 1444–1462.